Inorganic Chemistry

Article

pubs.acs.org/IC

γ-Cyclodextrin Cuprate Sandwich-Type Complexes

Abdulaziz A. Bagabas,*[,†,‡] Marco Frasconi,[‡] Julien Iehl,[‡] Brad Hauser,[‡] Omar K. Farha,[‡] Joseph T. Hupp,[‡] Karel J. Hartlieb,[‡] Youssry Y. Botros,[§,⊥,∥] and J. Fraser Stoddart*[,‡,#]

[†]Petrochemicals Research Institute (PRI) and [∥]National Center for Nano Technology Research, King Abdulaziz City for Science and Technology (KACST), P.O. Box 6086, Riyadh 11442, Saudi Arabia

[‡]Department of Chemistry and [§]Department of Materials Science and Engineering, Northwestern University, 2145 Sheridan Road, Evanston, Illinois 60208, United States

[⊥]Intel Labs, Building RNB-6-61, 2200 Mission College Boulevard, Santa Clara, California 95054, United States

[#]NanoCentury KAIST Institute and Graduate School of EEWS (WCU), Korea Advanced Institute of Science and Technology (KAIST), 373-1, Guseong Dong, Yuseong Gu, Daejeon 305-701, Republic of Korea

Supporting Information

ABSTRACT: Three structures, based on γ-cyclodextrin (γ-CD) and metal ions (Cu^{2+}, Li^+, Na^+, and Rb^+), have been prepared in aqueous and alkaline media and characterized structurally by single-crystal X-ray diffraction. Their dimeric assemblies adopt cylindrical channels along the *c* axes in the crystals. Coordinative and hydrogen bonding between the cylinders and the solvent molecules lead to the formation of two-dimensional sheets, with the identity of the alkali-metal ion strongly influencing the precise nature of the solid-state structures. In the case of the Rb^+ complex, coordinative bonding involving the Rb^+ ions leads to the formation of an extended two-dimensional structure. Nonbound solvent molecules can be removed, and gas isotherm analyses confirm the permanent porosity of these new complexes. Carbon dioxide (CO_2) adsorption studies show that the extended structure, obtained upon crystallization of the Rb^+-based sandwich-type dimers, has the highest CO_2 sequestration ability of the three γ-CD complexes reported.

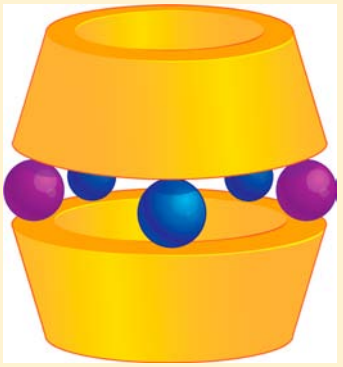

INTRODUCTION

Arrays of large, ordered, self-assembled structures based on naturally occurring, readily available, nontoxic, chemically stable cyclodextrins (α-CD, β-CD, and γ-CD), such as inclusion complexes,[1] mechanically interlocked molecules (rotaxanes and catenanes),[2] and metal−organic frameworks (MOFs),[3] are of prime importance because of their potential applications, for instance, in catalysis,[1n,j,4] enzyme models,[1a,j,n,4,5] drug delivery,[6] chemical sensing,[1a] gas storage,[3b] and enantioseparations.[7] All of these applications emerge from the ability of CDs to bind with other molecules by means of various bonding interactions—depending on the constitution of the CD, the guest molecules, and the solvent reaction medium—such as van der Waals, hydrophobic, hydrogen, and covalent bonds.[1−8] Several structural factors play key roles in determining the stability and type of the CD-based complexes. They include (1) the rigidity and the truncated cone shape of the CD molecule, resulting from the α-1,4-linkages between the D-glucopyranose rings and the intramolecular hydrogen bonds between them, (2) the size dependence, determined by the number of D-glucopyranose rings (the CD's wider cavity entrance is referred to as the secondary face because it bears secondary hydroxyl groups, while its narrower cavity entrance is referred to as the primary face because it bears primary hydroxyl groups), and (3) the hydrophobic nature of the interiors of the CD cavities, resulting from the alignment of the H(3) hydrogen atoms at the secondary face[1] and the H(5) hydrogen atoms near the primary face (Figure 1). These factors allow CDs (i) to form inclusion complexes with organic molecules in water and polar organic solvents, (ii) to serve as second-sphere coordination ligands[1c] for organometallic compounds, and (iii) to act as first-sphere coordination ligands[1n] for metal ions via their secondary and primary hydroxyl groups, as well as glucopyranosyl ring oxygen atoms. In addition, the possibility of functionalizing either all or one of the primary or secondary hydroxyl groups facilitates the modification of the physical and chemical properties of CDs, imposing better solubilities in low-polarity organic solvents, altering the inclusion ability for organic guests in aqueous media, and creating coordination sites for metal ions.[1−8]

Coordination of CDs to metal ions as first-sphere ligands as a result of deprotonation of the secondary hydroxyl groups has led to the production of sandwich-type complexes[8a,b] and cylindrical, extended structures,[8c−f] depending on the nature of the metal ion. Deprotonation, however, has to be performed at high pH in solution because of the high pK_a values, i.e., the weak acidity of CDs.[8a−f] There is only one previous example[8c] of the formation of a sandwich-type complex between Pb^{2+} ions and γ-CD in which two γ-CD tori are linked together by 16

Received: August 15, 2012
Published: February 22, 2013

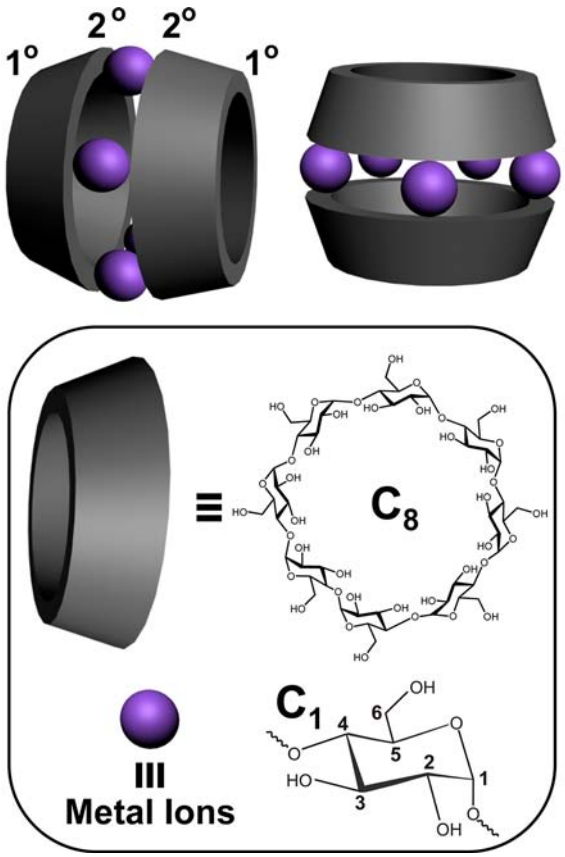

Figure 1. Channel and side views of the γ-cyclodextrin cuprate sandwich-type complexes. Structural formulas of γ-CD, with its C_8 symmetry, and the asymmetric C_1 α-1,4-linked D-glucopyranosyl residues.

Pb^{2+} ions to a form a dimer in the solid state; i.e., the complex does not form an extended structure upon crystallization. Recently, we reported[3] the formation of MOFs from γ-CD in aqueous solutions of alkali-metal cations in the presence of both nucleophilic and non-nucleophilic anions on vapor diffusion with methanol or ethanol. We also discovered[3c] that these so-called CD-MOFs have a high affinity for CO_2, which is adsorbed in a reversible manner as a result of both chemisorption and physisorption processes.

In this paper, we report the (i) crystal preparation, (ii) characterization by single-crystal and powder X-ray diffraction (PXRD), (iii) carbon dioxide (CO_2) adsorption isotherms, and (iv) thermogravimetric analyses (TGA) of the cylindrical, extended structures, obtained by deprotonation and complexation of the secondary hydroxyl groups of γ-CD to multinuclear Cu^{2+} and alkali-metal ions (Li^+, Na^+, or Rb^+), leading to sandwich-type complexes (Figure 1). The sandwich-type complex involving Rb^+ is unique insofar as it forms *an extended structure* in the solid state, a structural feature that allows it to exhibit enhanced CO_2 sequestration properties relative to the sandwich-type complexes formed with Li^+ and Na^+.

EXPERIMENTAL SECTION

Materials and Reagents. γ-Cyclodextrin (γ-CD, food-grade) was a gift from Wacker Chemie. Copper nitrate hemipentahydrate, lithium hydroxide monohydrate, sodium hydroxide, and rubidium hydroxide hydrate are commercially available from Sigma-Aldrich and were used without further purification.

Synthetic Procedure. Dark-blue crystals of the γ-cyclodextrin cuprate sandwich-type complexes were prepared by the reaction of γ-CD (2.594 g, 2.0 mmol), copper nitrate hemipentahydrate (0.697 g, 3.0 mmol), and the respective alkali hydroxide (12.0 mmol of LiOH or NaOH or 8.0 mmol of RbOH); these were all mixed as solids. An amount of deionized water (20.0 mL) was then added to dissolve this mixture at room temperature. Dark-blue solutions resulted, indicating complexation of the cupric ion. In order to obtain good-quality single crystals, the reaction solution (1.0 mL) was diluted five times by volume followed by diffusion of Me_2CO vapor. Crystals were observed to grow over the course of a few days up to 1 week.

Single-Crystal X-ray Crystallography. Single crystals suitable for X-ray crystallography were mounted on glass fibers using oil (Infineum v8512). All measurements were performed on a Bruker APEX-II CCD diffractometer with a Cu Kα IμS source. The data were collected at −173 °C, in 0.5° oscillations with 10 s exposures. The crystal-to-detector distance was 40.00 mm. The data were collected using a Bruker APEX2 detector and processed using *SAINTPLUS* from Bruker.[9] A multiscan absorption correction was applied. The data were corrected for Lorentz and polarization effects. The structures were solved, refined, and analyzed by direct methods and were expanded using Fourier techniques. Non-hydrogen atoms were refined anisotropically, while hydrogen atoms were included but not refined. The final cycle of full-matrix least-squares refinement was performed on F^2. Unweighted and weighted agreement factors (R values) were defined by $R(F) = \sum||F_o| - |F_c||/\sum|F_o|$ and $wR(F^2) = \{\sum[w(F_o^2 - F_c^2)^2]/\sum[w(F_o^2)^2]\}^{1/2}$, respectively. The weighting scheme was $w = 1/[\sigma^2(F_o^2) + (xP)^2 + yP]$ where $P = (F_o^2 + 2F_c^2)/3$. The weighting scheme was based on counting statistics and included a factor to downweigh the intense reflections. Plots of $\sum w(|F_o| - |F_c|)^2$ versus $|F_o|$, the reflection order in data collection, sin θ/λ, and various classes of indices showed no unusual trends. Neutral atom scattering factors were taken from Cromer and Waber.[10] Anomalous dispersion effects were included in F_c;[11] where values for Df′ and Df″ were those of Creagh and McAuley.[12] The values for the mass attenuation coefficients are those of Creagh and Hubbell.[13] All calculations were performed using the Bruker *SHELXTL3* crystallographic software package.[14] Diffuse, disordered solvent molecules could not be adequately modeled. The bypass procedure in *PLATON*[15] was used to remove the electronic contribution from these solvents. Because the exact solvent content is not known, the reported formula reflects only the atoms used in the refinement. The identity of the other anion could not be found and was "squeezed" out using the *SQUEEZE* routine from *PLATON*. Crystallographic parameters for all of the investigated structures are given in Table S1 (Supporting Information).

PXRD. Powder patterns were collected on a Bruker AXS APEX2 diffractometer equipped with a CCD detector and a Cu Kα IμS microfocus source with MX optics. Samples were mounted on nylon loops in a small amount of oil. Data were collected with an area detector as rotation frames over 180° in φ at 2θ values of 12°, 24°, 36°, and 48° exposed for 10 min for each frame. At a distance of 150 mm, the detector area covers 24° in 2θ. Overlapping sections of data were matched, and the resulting pattern was integrated using the Bruker APEX2 phase ID program. Powder pattern data were treated for amorphous background scatter (EVA 16, Bruker-AXS, 1996–2010).

NMR Spectroscopy. ^1H NMR spectra were recorded at 298 K on a Bruker Avance III 500 MHz spectrometer. Crystals were isolated by filtration and washed twice with MeOH (2 × 10 mL) to remove impurities. The crystals were dried in vacuo, dissolved in D_2O, and subjected to analysis by ^1H and ^{13}C NMR spectroscopy. As expected, the Cu^{2+} complexes showed paramagnetic NMR spectra. Therefore, a one-to-one assignment was not possible because of paramagnetic effects.

CO_2 Adsorption and Surface Area. Gas adsorption measurements were performed using an Autosorb 1-MP from Quantachrome Instruments (Boynton Beach, FL). Ultrahigh-purity-grade gases, obtained from Airgas Inc. (Radnor, PA), were used for all adsorption measurements without further purification. The sample was loaded

dx.doi.org/10.1021/ic301795j | Inorg. Chem. 2013, 52, 2854−2861

into a sample tube of known weight and activated at room temperature and dynamic vacuum for 24 h. After activation, the sample and tube were reweighed to obtain the precise mass. An attempt was made at obtaining a N_2 isotherm at 77 K on all samples, but none of them adsorbed N_2. CO_2 adsorption isotherms at 273 K were then measured. CO_2 isotherms were held at a constant 273 K in an ice–water bath. The surface area was determined using the slit-pore nonlocal density functional theory (NLDFT) model for CO_2 at 273 K on carbon from *AS1Win*, version 2.01, by Quantachrome Instruments.

TGA. TGA was performed on a Mettler-Toledo TGA/SDTA851e instrument. Samples (3–5 mg) in alumina pans were heated from 25 to 1000 °C at 10 °C/min under N_2.

RESULTS AND DISCUSSION

Design and Synthesis. The synthesis of γ-cyclodextrin cuprate sandwich-type complexes requires the cooperation of several key factors including (1) the ligation of metal ions to deprotonated as well as free hydroxyl groups of γ-CD, (2) the preferable binding of the counterion to the free hydroxyl groups of the opposing secondary faces of the γ-CD tori, (3) the presence of positively charged counterions, in some cases, coordinated only by solvent molecules, thus helping to bind the negatively charged sandwich-type complexes electrostatically, (4) the serving of some metal ions as bridges between two sandwich-type complexes, (5) the formation of hydrogen bonds [O–H···O], as a result of deprotonation of the γ-CD torus, and (6) the formation of hydrogen bonds between the solvent molecules of crystallization and the deprotonated and free hydroxyl groups of γ-CD. Thus, the metal ions are important structural components in forming strongly, highly directional metal–γ-CD bonds, leading to well-defined, rigid cylindrical geometries. Furthermore, the metal ions represent chromophore and redox centers, endow magnetic properties (in the case of Cu^{2+}), and act as sites for conducting reactions within these cylindrical structures.

Description of Structures. *$Li_4[Li_4(OH_2)_4Cu_4(\gamma\text{-}CDH_{-8})_2]$.* First, we investigated the formation of the sandwich-type complex of γ-CD with Cu^{2+} and Li^+ ions. According to the synthetic procedure, the γ-cyclodextrin cuprate lithium complex was prepared by combining γ-CD (2.0 equiv) with cupric nitrate (3.0 equiv) and lithium hydroxide (12.0 equiv) in aqueous solution. A dark-blue solution resulted, indicating complexation of the cupric ion. Then, single crystals, suitable for X-ray crystallography, were obtained by vapor diffusion of acetone into the blue solution for several days. Figure 2A shows a sandwich-type complex of the three symmetric independent $[Li_4(OH_2)_4Cu_4(\gamma\text{-}CDH_{-8})_2]^{4-}$ ions. Four Cu^{2+} ions are alternated with four Li^+ ions between two γ-CD ligands, where the metal ions are correlated by a noncrystallographic C_4 symmetry. The X-ray crystal structure of the Li–Cu-γ-CD assembly reveals that each Cu^{2+} ion resides in a distorted square-planar environment, as exemplified by the coordination environment of Cu2 in Figure 2B. This distortion in the Cu^{2+} coordination environment could be a consequence of the chair conformation of the glucopyranosyl ring, making the O2 atom more elevated than its vicinal O3 atom. The Cu^{2+} distorted square-planar environment was reported[8d,f] previously during the formation of sandwich-type complexes with α-CD and β-CD. On the other hand, each Li^+ ion exists in a distorted square-pyramidal coordination environment, where four secondary hydroxyl oxygen atoms form the base and the aqua ligand forms the outer apex of the sandwich-type complex (Figure 2C). A similar coordination environment was observed[8d] for Li^+ ions in a bimetallic α-CD sandwich-type

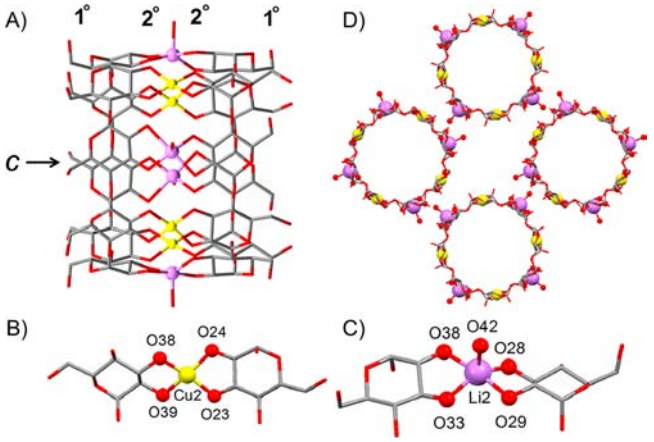

Figure 2. Stick representation of the γ-cyclodextrin cuprate lithium complex $[Li_4(OH_2)_4Cu_4(\gamma\text{-}CDH_{-8})_2]^{4-}$. (A) Side-on view showing the primary-to-secondary face orientation of the γ-CD rings in the solid-state structure. (B) Coordination sphere of the Cu^{2+} ions showing the distorted square-planar environment around the metal. (C) Coordination sphere of the Li^+ ion with the distorted square-pyramidal environment around the Li^+ ion. (D) Crystal packing of $(Li_4[Li_4(OH_2)_4Cu_4(\gamma\text{-}CDH_{-8})_2])_3 \cdot x$S (S = solvent) along the *c* axis. Color code: yellow, copper; purple, lithium; red, oxygen; gray, carbon.

complex with Cu^{2+} ions. The apex aqua ligand coordinated to Li^+ ion, however, is inside the cavity of the bimetallic α-CD sandwich-type complexes formed with Li^+ and Fe^{2+}, Li^+, and Mn^{2+} and Li^+ and VO^{2+}, Li^+, and Bi^{3+},[8f] and also in the bimetallic β-CD sandwich-type complex formed with Li^+ and Cu^{2+}.[8f]

The charge on the anionic dimer is offset by four Li^+ ions within and outside the γ-CD cavity. In addition, some weakly bound solvent molecules exist in the interior of the anionic sandwich-type complex as a result of the absence of ligands coordinated to the metal ions within the cavity of the dimer. Four anionic sandwich-type complexes are regularly packed in a roll-of-coins-type mode with the help of the Li^+ ions and [O–H···O] bonds between the sandwich-type anions and the solvent molecules (Table S2, Supporting Information). The anionic sandwich-type complexes arrange themselves in a regular tetragonal rod packing along the *c* axis (Figure 2D). Thus, electrostatic attraction forces and the hydrogen bonds act as "glue" for gathering the negatively charged sandwich-type cylinders. This kind of packing is similar to that observed[8d] in the α-CD complex with K^+ ions. Furthermore, the γ-cyclodextrin cuprate lithium complex crystallizes in a primitive tetragonal crystal system with space group $P42(1)2$ (Table S1, Supporting Information), making it more symmetrical than either the primitive monoclinic $P2_1$ α-CD homologue or the sphenoidal orthorhombic $P2_12_12_1$ β-CD homologue. However, the total potential solvent-accessible void volume is 8997 Å^3, corresponding to 30.6% of the crystal volume (29394 Å^3) for the γ-cyclodextrin cuprate lithium complex, which is responsible of the lower density of 1.133 g/cm^3, compared to 1.402 g/cm^3 for the α-CD homologue[8d] and 1.221 g/cm^3 for the β-CD[8f] homologue, which possess smaller solvent-accessible void volumes.

As-synthesized and activated (solvent removed) samples of $Li_4[Li_4(OH_2)_4Cu_4(\gamma\text{-}CDH_{-8})_2]$ were analyzed for their thermal behavior by TGA (Supporting Information). The as-synthesized $Li_4[Li_4(OH_2)_4Cu_4(\gamma\text{-}CDH_{-8})_2]$ sample was stable up to 200 °C—an observation that was also evident in the case of the

dx.doi.org/10.1021/ic301795j | *Inorg. Chem.* 2013, 52, 2854–2861

activated sample—followed by a rapid, large mass loss in the sample, which most likely coincides with destruction of the overall network. The thermal stability comes from the strong hydroxyl−metal bonding formed between the independent γ-CD rings. Prior to network destruction, the Li−Cu-γ-CD assembly loses 25 wt % owing to removal of the guest solvent molecules. The magnitude of solvent loss matches well with the crystallographically determined void volume in the structure of $(Li_4[Li_4(OH_2)_4Cu_4(\gamma\text{-}CDH_{-8})_2])_3{\cdot}xS$ (S = solvent).

Gas isotherm analysis was carried out on the crystalline material (Supporting Information). Attempts to study the adsorption of N_2 at 77 K yielded no evidence for uptake of gas molecules. The closely packed cylinders in the solid state are believed to prevent adsorbates from gaining access to the internal pores at this low temperature. By contrast, CO_2 isotherms at 273 K demonstrate that the porosity of the assemblies is accessible after removal of the nonbound solvent. The observed uptake of CO_2 (and not N_2) can be attributed to two factors. They are (i) an increase in the thermal motion at higher temperatures and (ii) a higher affinity between the assembly and CO_2 molecules. A previous study[16] with a CD-based polymer also showed little N_2 uptake. The activated $Li_4[Li_4(OH_2)_4Cu_4(\gamma\text{-}CDH_{-8})_2]$ sample exhibited an uptake of 40 cm^3/g CO_2 at 1 bar and a NLDFT surface area of 370 m^2/g, as estimated from the CO_2 gas isotherm data collected. The Li−Cu-γ-CD assembly demonstrated strong adsorbent binding with irreversible hysteresis in the desorptive branch of the CO_2 isotherm, most likely a consequence of the small, constricted pores and strong binding to Cu^{2+} and alkali-metal cations. This irreversible sorption behavior, however, makes this assembly an unlikely candidate for CO_2 capture applications because these applications usually require reversible adsorption and desorption of CO_2.

It appears from the PXRD patterns that the samples show very intense low-angle peaks (in the 2θ range of 0−20°), followed by a rapid drop-off of the diffraction at higher angles ($2\theta > 20°$). The large, broad peaks at higher angles come from the background scattering of the loop in which the samples were mounted (Supporting Information). This phenomenon is similar to that observed for single crystals of these materials, where there were intense peaks at low angles but hardly any diffraction at high angles. This observation indicates a lack of long-range order, which apparently still holds in the bulk powder as well as in the single crystal. The PXRD patterns of as-synthesized and activated samples of $(Li_4[Li_4(OH_2)_4Cu_4(\gamma\text{-}CDH_{-8})_2])_3$ were identical, an observation that confirmed the integrity of the Li−Cu-γ-CD assembly upon removal of the solvent guest molecules.

$[Na_4Cu_4(\gamma\text{-}CDH_{-3})_4(OH_2)]$. Second, we investigated the formation of the sandwich-type complex of γ-CD with Cu^{2+} and Na^+ ions. According to the synthetic procedure, the γ-cyclodextrin cuprate sodium complex was prepared by combining γ-CD (2.0 equiv) with cupric nitrate (3.0 equiv) and sodium hydroxide (12.0 equiv) in aqueous solution. A dark-blue solution resulted, indicating complexation of the cupric ion. Then, single crystals suitable for X-ray crystallography were obtained by vapor diffusion of acetone into the blue solution for several days. The X-ray crystal structure of the Na−Cu-γ-CD assembly reveals that the γ-cyclodextrin cuprate sodium complex crystallizes in a triclinic crystal system with space group *P*1, making it less symmetric than the monoclinic $P2_1$ α-cyclodextrin cuprate sodium complex,[8d] the trigonal *P*312 α-CD sandwich-type complex with VO^{2+} and Na^+, and the orthorhombic *C*222 α-CD sandwich-type complex with Bi^{3+} and Na^+.[8c] The total potential solvent-accessible void volume is 3648.9 $Å^3$ in the γ-cyclodextrin cuprate sodium complex, representing 42.4% of the crystal volume (8615.5 $Å^3$), which makes its density (1.064 g/cm^3) less than those for the α-CD complexes (i) with Cu^{2+} and Na^+ (1.443 g/cm^3),[8d] (ii) with VO^{2+} and Na^+ (1.453 g/cm^3), and (iii) with Bi^{3+} and Na^+ (1.765 g/cm^3).[8c] The γ-cyclodextrin sodium−copper sandwich-type complex contains two unsymmetrically neutral sandwich-type complexes connected by a coordination bond between the free secondary hydroxyl group O3, labeled as O68 of the glucopyranosyl ring of one sandwich-type complex (SC1), and the Na3A$^+$ ion, located between the two Cu^{2+} ions in the other sandwich-type complex (SC2), as depicted in Figure 3A.

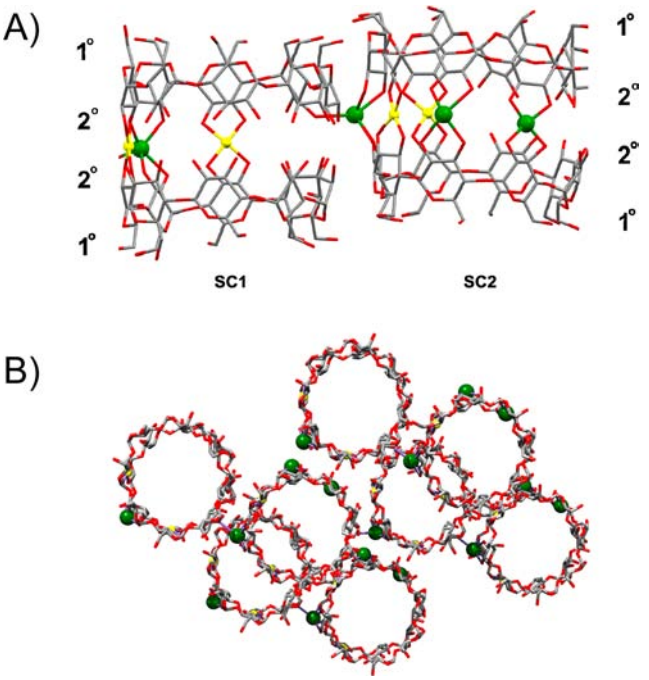

Figure 3. (A) Crystal structures of the two unsymmetrical sandwich-type complexes of $[Na_4Cu_4(\gamma\text{-}CDH_{-3})_4(OH_2)]$. (B) Crystal packing viewed down the axes of the sandwich-type dimers, revealing an overlap of the complexes, resulting in lower porosity. Color code: yellow, copper; green, sodium; red, oxygen; gray, carbon.

There are four Cu^{2+} ions equally distributed between the two sandwich-type complexes. The Na^+ ions, on the other hand, are not evenly distributed; one ion resides in SC1 and three in SC2. The total charge of the cations is 12+. Therefore, the four γ-CD tori anions have 12− charges for neutralizing the two sandwich-type complexes, with an average of 3− charges per γ-CD torus anion. However, because cations are not equally distributed between the two sandwich-type complexes, SC1 bears a charge of 7−, while SC2 carries a charge of 5−. The distribution of the negative charge between the two sandwich-type complexes, alternatively, can be thought of as equally distributed, where each dimer carries a charge of 6−. In this manner, the net charge of SC1 is 1− because the total charge of the cations is 5+, while the net charge of SC2 is 1+ because the total charge of the cations is 7+. This unequal distribution of the negative charges could be responsible for the Na3A−O68 connecting bridge between SC1 and SC2 (Figure S1-C, Supporting Information). Each Cu^{2+} ion lies in a distorted square-planar

dx.doi.org/10.1021/ic301795j | Inorg. Chem. 2013, 52, 2854−2861

coordination environment because of its ligation to two O2 and two O3 of the opposing secondary face of the γ-CD tori, as it is represented by the coordination environment of Cu2A (Figure S1-A, Supporting Information). Such a distortion of the Cu^{2+} ion was observed in its bimetallic α-CD sandwich-type complex with Na^+ ions.[8d] Each Na^+ ion has its own distinctive coordination environment. The $Na1^+$ ion in SC1 has a distorted square-pyramidal coordination environment, whereas the base is made up by the four secondary hydroxyl oxygen atoms of the facing γ-CD rims and the coordinated aqua ligand forms the apex outside the cavity of SC1 (Figure S1-B, Supporting Information). This distortion forces the $Na1^+$ ion to lie above the base plane of its square pyramid by 0.882 Å. The $Na3A^+$ ion resides also in a distorted square-pyramidal environment. However, the apex of this square pyramid is occupied by the secondary hydroxyl O3, labeled O68, which results in bridging SC1 and SC2 (Figure S1-C, Supporting Information) and drawing the $Na3A^+$ ion by 1.191 Å above the base plane of its square pyramid toward SC1.

Such pulling of the $Na3A^+$ ion may provide evidence in support of our hypothesis of a 1− net charge for SC1 and a net charge for SC2. A distorted square-planar coordination environment was observed for both the $Na1A^+$ and $Na2A^+$ ions, where the base is made up of secondary hydroxyl oxygen atoms. Because the $Na1A^+$ and $Na2A^+$ ions are not separated by a γ-cyclodextrin cuprate moiety, the repulsion between the two positively charged Na^+ ions is observed by the movement of $Na1A^+$ toward the cavity of SC2 and its residence by 0.35 Å below the base plane of its square-planar geometry and the movement of $Na2A^+$ above the base plane of its square-planar geometry by 0.717 Å (Figure S1-D, Supporting Information). Hydrogen bonds also contribute significantly to the stabilization of SC1 and SC2 (Table S3, Supporting Information). The SC1−SC2 pair sandwich-type complex packs into a two-dimensional sheet along the *c* axis. The sandwich-type pairs along the sheet are connected by hydrogen bonds (Figure 3). The observed topography of the bimetallic γ-CD complex with Cu^{2+} and Na^+ is unique in comparison to the bimetallic alternate placement of the α-CD sandwich-type complexes of Na^+ and Cu^{2+},[8d] Na^+ and VO^{2+}, and Na^+ and Bi^{3+}.[8c]

TGA of the as-synthesized sample of $[Na_4Cu_4(\gamma\text{-}CDH_{-3})_4(OH_2)]$ showed stability up to 200 °C, while the activated sample began to degrade at 180 °C, followed by a quick, large mass loss in the samples, which might be a result of destruction of the overall network. Before network destruction, the Na−Cu-γ-CD assembly loses 16 wt %, in the form of guest solvent molecules (Supporting Information). The magnitude of solvent loss matches well with the crystallographically determined void volume in the structure of $[Na_4Cu_4(\gamma\text{-}CDH_{-3})_4(OH_2)]$.

Gas isotherm analysis was carried out on the crystalline material. The activated $[Na_4Cu_4(\gamma\text{-}CDH_{-3})_4(OH_2)]$ sample took up 14 cm^3/g of CO_2 at 1 bar with an NLDFT surface area of 130 m^2/g, as estimated from the CO_2 gas isotherm data collected. As in the case of the Li−Cu-γ-CD assembly, the Na−Cu-γ-CD assembly demonstrated strong adsorbent binding with irreversible hysteresis in the desorptive branch of the CO_2 isotherm, owing to its small, constricted pores and strong binding to Cu^{2+} and alkali-metal cations (Supporting Information). The irreversible gas adsorption behavior makes this assembly an unlikely candidate for CO_2 capture applications because these applications usually require reversible adsorption and desorption of CO_2 without requiring heat to remove the adsorbate.

The PXRD patterns of the as-synthesized and activated samples of $[Na_4Cu_4(\gamma\text{-}CDH_{-3})_4(OH_2)]$ were identical, an observation that confirmed that the structure of the Na−Cu-γ-CD assembly remains intact upon removal of the solvent guest molecules (Supporting Information).

$[Rb_6Cu_9(\gamma\text{-}CDH_{-12})_2(OH_2)]$. Finally, we investigated the formation of the sandwich-type complex of γ-CD with Cu^{2+} and Rb^+ ions. The γ-cyclodextrin cuprate rubidium complex was synthesized from an aqueous solution of γ-CD (2.0 equiv), cupric nitrate (3.0 equiv), and rubidium hydroxide (8.0 equiv). Single crystals, suitable for X-ray crystallography, were obtained by vapor diffusion of acetone into the blue solution for several days. The X-ray crystal structure of the Rb−Cu-γ-CD assembly reveals that the complexes are bridged by two symmetrically correlated $Rb2^+$ ions, which reside in a distorted square antiprism with a coordination number of 8. The two symmetrically bridged sandwich-type complexes of $[Rb_6Cu_9(\gamma\text{-}CDH_{-12})_2(OH_2)]$ are shown in Figure 4A. Each

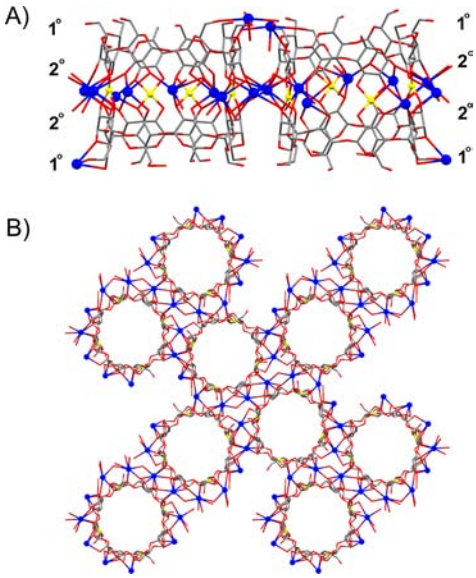

Figure 4. (A) Stick representation of the extended structure of the two symmetrical sandwich-type complexes of $[Rb_6Cu_9(\gamma\text{-}CDH_{-12})_2(OH_2)]$ and (B) view of the packing of $[Rb_6Cu_9(\gamma\text{-}CDH_{-12})_2(OH_2)]$ along the *c* axis. Color code: yellow, copper; blue, rubidium; red, oxygen; gray, carbon.

sandwich-type complex has four Cu^{2+} ions and six Rb^+ ions, bridging the torus of the two opposing secondary faces of γ-CD ligands. Hydrogen bonding also plays a key role in stabilizing and binding each dimer (Table S4, Supporting Information). Each Cu^{2+} ion resides in a distorted square-planar environment, made up by two secondary hydroxyl O2 atoms and two secondary hydroxyl O3 atoms of the facing glucopyranosyl rings (Figure S2, Supporting Information). This distortion of the coordination environment of Cu^{2+} ions has also been reported[8d] for the homologous α-CD sandwich-type complex with unsandwiched Rb^+ counterions. The O2 and O3 atoms, ligated to a Cu^{2+} ion, serve as a bridge to the neighboring Rb^+ ion(s), residing in the same dimer or connecting the dimer to an adjacent complex. Such a role for the O2 and O3 atoms has been reported previously[8c] for the bimetallic α-CD sandwich-type complexes of Cu^{2+} and Na^+,[8d] Fe^{2+} and Li^+, VO^{2+} and Na^+,

dx.doi.org/10.1021/ic301795j | Inorg. Chem. 2013, 52, 2854−2861

and Bi^{3+} and Na^+, as well as for the γ-CD sandwich-type complex with Pb^{2+}.[8e] The role of the O2 and O3 atoms in bridging is responsible for the limitation of the number of hydrogen bonds to two (Table S4, Supporting Information). The coordination number of Rb^+ ions ranges between 4 and 8, depending on their relative positions within the dimer and their role in binding the two γ-CD tori in a sandwich-type complex as well as bridging between the sandwich-type complexes (Figure S3, Supporting Information), creating an *extended solid-state structure*. The primary hydroxyl oxygen O6 and the glucopyranosyl ring oxygen atoms are coordinated to the Rb4$^+$ ion, which has been observed previously[3] in CD-MOFs constructed from γ-CD and alkali-metal (Na^+, K^+, Rb^+, or Cs^+) hydroxides, halides, carbonates, or carboxylates and in the first-sphere coordination of Ca^{2+} by α-CD[8g] and β-CD.[8h] $[Rb_6Cu_9(\gamma\text{-}CDH_{-12})_2(OH_2)]$ packs in two-dimensional sheets (Figure 4B), where each sheet is connected to its adjacent sheets by hydrogen bonds, as observed in the packing mode along the *a* axis. The γ-cyclodextrin cuprate rubidium complex crystallizes in a tetragonal crystal system with space group *P*4(2)2(1)2, making it more symmetric than the orthorhombic 222-D_2 α-cyclodextrin cuprate rubidium complex.[8d] The total potential solvent-accessible void volume is 13063.7 Å^3 in the γ-cyclodextrin cuprate rubidium complex, representing 35.9% of the crystal volume (36375.5 Å^3). The density of the γ-cyclodextrin cuprate rubidium complex (1.347 g/cm^3) is less than that for its α-CD homologue complex (1.578 g/cm^3).

As-synthesized and activated samples of $[Rb_6Cu_9(\gamma\text{-}CDH_{-12})_2(OH_2)]$ were subjected to TGA, showing stability up to 200 °C (Figure 5A). The activated sample exhibited an uptake of 67 cm^3/g of CO_2 at 1 bar and a NLDFT surface area of 650 m^2/g, as estimated from the CO_2 gas isotherm data collected (Figure 5B). To confirm the sample integrity upon activation, PXRD analyses were carried out. The PXRD patterns (Figure 5C) of the as-synthesized sample match very well with the activated $[Rb_6Cu_9(\gamma\text{-}CDH_{-12})_2(OH_2)]$, showing that the framework of $[Rb_6Cu_9(\gamma\text{-}CDH_{-12})_2(OH_2)]$ remains intact upon removal of the occluded solvent.

Comparison of the Structures. A comparison of all three solid-state structures reveals that, in the Li^+ and Rb^+ complexes, which are highly symmetric, their γ-CD dimers pack directly on top of each other, resulting in porous structures. In the Na^+ complex, on the other hand, which is not symmetric—crystallizing in a space group *P*1—the γ-CD dimers do not stack above one another (Figure 3B) and, as a consequence, display significantly reduced porosity. This finding is also reflected in the results obtained from CO_2 adsorption studies, which have revealed that the more symmetric Li^+ and Rb^+ complexes have higher gas uptake properties.[17] In addition, we believe that the gas uptake, in the case of the Rb^+ complex, is enhanced because it is the only sandwich-type complex that crystallizes to form *an extended structure*. These gas uptake studies also reveal that CO_2 adsorption is not completely reversible, whereas the related CD-MOFs display[3c] fully reversible CO_2 uptake. Another notable difference between these sandwich-type complexes and the CD-MOFs is the lack of a rapid uptake of CO_2 at low partial pressures, which, in the case of CD-MOF-2, has been ascribed[3c] to a chemisorption process. This reversible chemisorption is believed to be a consequence of the reaction between CO_2 and the free primary hydroxyl groups of γ-CD: moreover, it was observed in the presence of hydroxide counterions as well as non-nucleophilic anions, such as fluoride. In the case of the γ-CD sandwich-type

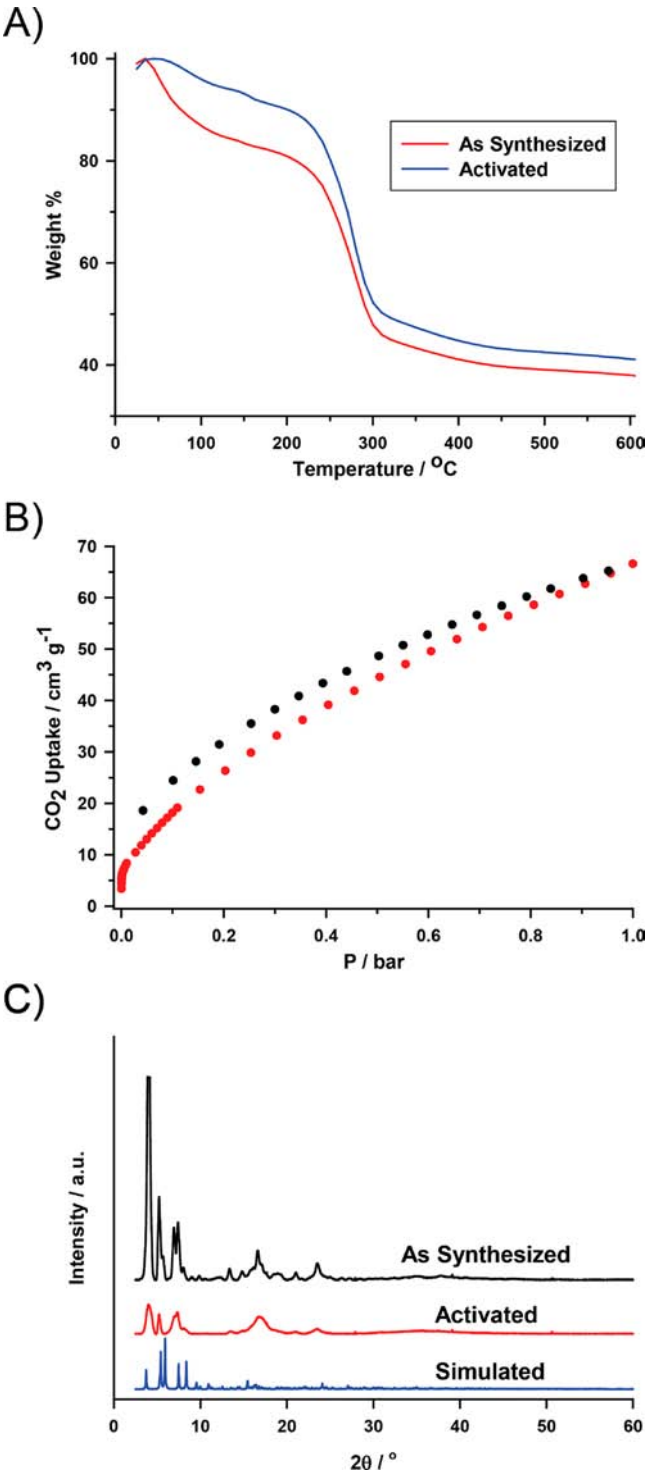

Figure 5. (A) Thermograms of $[Rb_6Cu_9(\gamma\text{-}CDH_{-12})_2(OH_2)]$ for both as-synthesized (red) and activated (blue) forms, (B) adsorption (black dots) and desorption (red dots) isotherms measured on activated $[Rb_6Cu_9(\gamma\text{-}CDH_{-12})_2(OH_2)]$ for the uptake of CO_2, and (C) PXRD patterns of as-synthesized (black) and activated (red) $[Rb_6Cu_9(\gamma\text{-}CDH_{-12})_2(OH_2)]$.

complexes, the lack of a rapid rise in CO_2 uptake at low partial pressures suggests that chemisorption does not occur and that physisorption is the major source of CO_2 uptake taking place within these complexes. We speculate that the partially reversible nature of CO_2 adsorption observed for the sandwich-type complexes reported here results from the

dx.doi.org/10.1021/ic301795j | Inorg. Chem. 2013, 52, 2854−2861

presence of an excess of alkali-metal cations and Cu^{2+} dications, most likely in the form of their hydroxides. The presence of Cu^{2+}, which is not coordinated to γ-CD, has only been confirmed in *the extended structure* of the Rb^+ complex, while noncoordinated Li^+ has been observed in the $Li_4[Li_4(OH_2)_4Cu_4(\gamma\text{-}CDH_{-8})_2]$ structure. Copper(II) and lithium hydroxides react with CO_2 to form their respective carbonates in an irreversible manner. The most efficient CO_2 uptake, which is observed for the Rb^+ complex, is similar to that recorded[3c] for CD-MOF-2, which also incorporates Rb^+ ions. We speculate that this increased CO_2 uptake is a consequence of the formation of *an extended structure* upon crystallization. It is important to note that CO_2 uptake has only been observed in crystalline forms of CD-MOFs and the sandwich-type complexes we report here. γ-CD alone and amorphous powders obtained upon grinding of CD-MOFs do not adsorb CO_2, pointing to the crystalline structure being critical for the gas uptake properties of these CD complexes.

CONCLUSIONS

Deprotonation of γ-CD is readily accomplished in highly basic, aqueous media. When the resultant anionic, truncated cone γ-CD ligand is crystallized in the presence of transition- and alkali-metal ions, rigid cylindrical solid-state structures are obtained in which coordinative bonding is supplemented by hydrogen bonds. The identity of the metal ions and hydrogen bonding dictate the direction and assembly of the cylindrical structures to produce the final solid-state structures. We have shown that the constitutions of these solid-state structures have a strong influence on their materials chemistry, particularly with respect to their mode of uptake of CO_2. Metal ion complexes with CDs, which result in *extended solid-state structures*, could offer a cheap, sustainable, and green solution to the sequestration of CO_2.

ASSOCIATED CONTENT

Supporting Information

Crystal structure and hydrogen-bonding data, coordination environments, TGA, CO_2 adsorption, and PXRD, and an additional reference. This material is available free of charge via the Internet at http://pubs.acs.org.

AUTHOR INFORMATION

Corresponding Author

*E-mail: abagabas@hotmail.com (A.A.B.), stoddart@northwestern.edu (J.F.S.).

Notes

The authors declare no competing financial interest.

ACKNOWLEDGMENTS

The authors thank Dr. Amy Sarjeant, Charlotte C. Stern, and the personnel in the Integrated Molecular Structure Education and Research Center at Northwestern University (NU) for their assistance in the collection of X-ray crystallographic data. We also thank Anthea Blackburn for her help in solving and refining the crystal structures of the γ-CD complexes with Cu^{2+} and Rb^+. The research at NU was sponsored by the National Center for Nano Technology at KACST in Saudi Arabia. The authors thank Dr. Turki M. Al-Saud and Dr. Soliman H. Alkhowaiter at KACST for their generous support of this program of research at NU. In addition, J.T.H. and O.K.F. thank the U.S. Department of Energy for support under the auspices of Grant DE-FG02-08ER15967.

REFERENCES

(1) (a) Saenger, W. *Angew. Chem., Int. Ed. Engl.* **1980**, *19*, 344−362. (b) Harada, A.; Takahashi, S. *J. Chem. Soc., Chem. Commun.* **1984**, 645−646. (c) Ashton, P. R.; Slawin, M. Z. A.; Stoddart, J. F.; Williams, D. J. *Angew. Chem., Int. Ed. Engl.* **1985**, *24*, 786−787. (d) Matsue, T.; Kato, T.; Akiba, U.; Osa, T. *Chem. Lett.* **1985**, 1825−1828. (e) Harada, A.; Takahashi, S. *J. Chem. Soc., Chem. Commun.* **1986**, 1229−1230. (f) Harada, A.; Hu, Y.; Yamamoto, S.; Takahashi, S. *J. Chem. Soc., Dalton Trans.* **1988**, 729−732. (g) Kobayashi, N.; Opallo, M. *J. Chem. Soc., Chem. Commun.* **1990**, 477−479. (h) Odagaki, Y.; Hirotsu, K.; Higuchi, T.; Harada, A.; Takahashi, S. *J. Chem. Soc., Perkin Trans. 1* **1990**, 1230−1231. (i) Isnin, R.; Salam, C.; Kaifer, E. A. *J. Org. Chem.* **1991**, *56*, 35−41. (j) Wenz, G. *Angew. Chem., Int. Ed. Engl.* **1994**, *33*, 803−822. (k) Castro, R.; Cuadrado, I.; Alonso, B.; Casado, M. C.; Morán, M.; Kaifer, E. A. *J. Am. Chem. Soc.* **1997**, *119*, 5760−5761. (l) Yoshida, K.; Shimomura, T.; Ito, K.; Hayakawa, R. *Langmuir* **1999**, *15*, 910−913. (m) Jiao, H.; Goh, H. S.; Valiyaveettil, S. *Macromolecules* **2002**, *35*, 1980−1983. (n) Engeldinger, E.; Armspach, D.; Matt, D. *Chem. Rev.* **2003**, *103*, 4147−4174. (o) Ogoshi, T.; Harada, A. *Sensors* **2008**, *8*, 4961−4982. (p) Casas-Solvas, M. J.; Ortiz-Salmerón, E.; Fernández, I.; García-Fuentes, L.; Santoyo-González, F.; Vargas-Berenguel, A. *Chem.—Eur. J.* **2009**, *15*, 8146−8162. (q) Zhao, Y.-L.; Benítez, D.; Yoon, I. J.; Stoddart, J. F. *Chem.—Asian. J.* **2009**, *4*, 446−456. (r) Chen, G.; Jiang, M. *Chem. Soc. Rev.* **2011**, *40*, 2254−2266.

(2) (a) Ogino, H. *J. Am. Chem. Soc.* **1981**, *103*, 1303−1304. (b) Ogino, H.; Ohata, K. *Inorg. Chem.* **1984**, *23*, 3312−3316. (c) Stoddart, J. F. *Angew. Chem., Int. Ed. Engl.* **1992**, *31*, 846−848. (d) Armspach, D.; Ashton, P. R.; Moore, C. P.; Spencer, N.; Stoddart, J. F.; Wear, T. J.; Williams, D. J. *Angew. Chem., Int. Ed. Engl.* **1993**, *32*, 854−858. (e) Macartney, H. D.; Waddling, A. C. *Inorg. Chem.* **1994**, *33*, 5912−5919. (f) Armspach, D.; Ashton, P. R.; Ballardini, R.; Balzani, V.; Godi, A.; Moore, C. P.; Prodi, L.; Spencer, N.; Stoddart, J. F.; Tolley, M. S.; Wear, T. J.; Williams, D. J.; Stoddart, J. F. *Chem.—Eur. J.* **1995**, *1*, 33−55. (g) Nepogodiev, A. S.; Stoddart, J. F. *Chem. Rev.* **1998**, *98*, 1959−1976. (h) Harada, A. *Acc. Chem. Res.* **2001**, *34*, 456−464. (i) Lim, W. C.; Sakamoto, S.; Yamaguchi, K.; Hong, J.-I. *Org. Lett.* **2004**, *6*, 1079−1082. (j) Fleury, G.; Brochon, C.; Schlatter, G.; Bonnet, G.; Lapp, A.; Hadziioannou, G. *Soft Matter* **2005**, *1*, 378−385. (k) Murakami, H.; Kawabuchi, A.; Matsumoto, R.; Ido, T.; Nakashima, N. *J. Am. Chem. Soc.* **2005**, *127*, 15891−15899. (l) Mezzina, E.; Fanì, M.; Ferroni, F.; Franchi, P.; Menna, M.; Lucarini, M. *J. Org. Chem.* **2006**, *71*, 3773−3777. (m) Daniell, W. H.; Klotz, E. F. J.; Odell, B.; Claridge, T. W. D.; Anderson, L. H. *Angew. Chem., Int. Ed.* **2007**, *46*, 6845−6848. (n) Sakamoto, K.; Takashima, Y.; Yamaguchi, H.; Harada, A. *J. Org. Chem.* **2007**, *72*, 459−465. (o) Sugiyama, J.; Tomita, I. *Eur. J. Org. Chem.* **2007**, 4651−4653. (p) Zhao, Y.-L.; Dichtel, R. W.; Trabolsi, A.; Saha, S.; Aprahamian, I.; Stoddart, J. F. *J. Am. Chem. Soc.* **2008**, *130*, 11294−11296. (q) Taira, T.; Suzaki, Y.; Osakada, K. *Chem. Lett.* **2008**, *37*, 182−183.

(3) (a) Smaldone, R. A.; Forgan, R. S.; Furukawa, H.; Gassensmith, J. J.; Slawin, A. M. Z.; Yaghi, O. M.; Stoddart, J. F. *Angew. Chem., Int. Ed.* **2010**, *49*, 8630−8634. (b) Holman, K. T. *Angew. Chem., Int. Ed.* **2011**, *50*, 1228−1230. (c) Gassensmith, J. J.; Furukawa, H.; Smaldone, R. A.; Forgan, R. S.; Botros, Y. Y.; Yaghi, O. M.; Stoddart, J. F. *J. Am. Chem. Soc.* **2011**, *133*, 15312−15315. (d) Forgan, R. S.; Smaldone, R. A.; Gassensmith, J. J.; Furukawa, H.; Cordes, D. B.; Li, Q.; Wilmer, C. E.; Botros, Y. Y.; Snurr, R. Q.; Slawin, A. M. Z.; Stoddart, J. F. *J. Am. Chem. Soc.* **2012**, *134*, 406−417.

(4) (a) Bricout, H.; Hapiot, F.; Ponchel, A.; Tilloy, S.; Monflier, E. *Sustainability* **2009**, *1*, 924−945. (b) Marinescu, L.; Bols, M. *Curr. Org. Chem.* **2010**, *14*, 1380−1398. (c) Woggon, W. D. *Curr. Org. Chem.* **2010**, *14*, 1362−1379. (d) Braga, S. S. *Curr. Org. Chem.* **2010**, *14*, 1356−1361. (e) Armspach, D.; Matt, D. *C. R. Chim.* **2011**, *14*, 135−148.

(5) Breslow, R.; Dong, S. D. *Chem. Rev.* **1998**, *98*, 1997−2012.

(6) (a) Zouvelekis, D.; Yannakopoulou, K.; Mavridis, I. M.; Antoniadou-Vyza, E. *Carbohydr. Res.* **2002**, *337*, 1387−1395. (b) Hirayama, F.; Uekama, K. *Adv. Drug Delivery Rev.* **1999**, *36*, 125−141. (c) Paulidou, A.; Maffeo, D.; Yannakopoulou, K.; Mavridis, I. M. *Carbohydr. Res.* **2008**, *343*, 2634−2640.
(7) Ohta, N.; Fuyuhiro, A.; Yamanari, K. *Inorg. Chem.* **2010**, *49*, 9122−9124.
(8) (a) Fuchs, R.; Habermann, N.; Klüfers, P. *Angew. Chem., Int. Ed. Engl.* **1993**, *32*, 852−854. (b) Klüfers, P.; Schuhmacher, J. *Angew. Chem., Int. Ed. Engl.* **1994**, *33*, 1863−1865. (c) Nicolis, I.; Coleman, A. W.; Charpin, P.; de Rango, C. *Acta Crystallogr., Sect. B: Struct. Sci.* **1996**, *52*, 122−130. (d) Klüfers, P.; Piotrowski, H.; Uhlendorf, J. *Chem.—Eur. J.* **1997**, *3*, 601−608. (e) Nicolis, I.; Coleman, A. W.; Selkti, M.; Villain, F.; Charpin, P.; de Rango, C. *J. Phys. Org. Chem.* **2001**, *14*, 35−37. (f) Geißelmann, A.; Klüfers, P.; Kropfgans, C.; Mayer, P.; Piotrowski, H. *Angew. Chem., Int. Ed.* **2005**, *44*, 924−927. (g) Benner, K.; Ihringer, J.; Klüfers, P.; Marinov, D. *Angew. Chem., Int. Ed.* **2006**, *45*, 5818−5822. (h) Li, S.-L.; Lan, Y.-Q.; Ma, J.-F.; Yang, J.; Zhang, M.; Su, Z.-M. *Inorg. Chem.* **2008**, *47*, 2931−2933.
(9) *APEX2*, V2.1-4; Bruker Analytical X-ray Instruments: Madison, WI, 2007.
(10) Cromer, D. T.; Waber, J. T. *Tables for X-ray Crystallography*; The Kynoch Press: Birmingham, England, 1974; Vol. *IV*.
(11) Ibers, J. A.; Hamilton, W. C. *Acta Crystallogr.* **1964**, *17*, 781−782.
(12) Creagh, D. C.; McAuley, W. J. *International Tables for Crystallography*; Kluwer Academic Publishers: Boston, 1992; Vol. *C*.
(13) Creagh, D. C.; Hubbell, J. H. *International Tables for Crystallography*; Kluwer Academic Publishers: Boston, 1992; Vol. *C*.
(14) *SHELXTL*, version 6.14; Bruker Analytical X-ray Instruments: Madison, WI, 2003.
(15) Van Der Sluis, P.; Spek, L. A. *Acta Crystallogr.* **1990**, *46*, 194−201.
(16) Mhlanga, S. D.; Mamba, B. B.; Krause, R. W.; Malefetse, T. J. *J. Chem. Technol. Biotechnol.* **2007**, *82*, 382−388.
(17) Although we have obtained a high level of correlation between the experimental and simulated PXRD data for both the Li^+ and Rb^+ complexes, we do not observe a match for the Na^+ complex.